Adaptive Radar Detection Algorithm Based on an Autoregressive GARCH-2D Clutter Model

Juan P. Pascual, Nicolás von Ellenrieder, *Member, IEEE*, Martín Hurtado, *Member, IEEE*, and Carlos H. Muravchik, *Senior Member, IEEE*

***Abstract*—We propose a model for radar clutter that combines an autoregressive (AR) process with a two-dimensional generalized autoregressive conditional heteroscedastic (GARCH-2D) process. Based on this model, we derive an adaptive detection test, called AR-GARCH-2D detector, for a target with known Doppler frequency and unknown complex amplitude. Using real radar data, we evaluate its performance for different model orders, and we use a model selection criteria to choose the best fit to the data. The resulting detector is not the constant false alarm rate (CFAR) with respect to the process coefficients, but we show that in practical situations it is very robust. Finally, we compare the AR-GARCH-2D detector performance with the performance of the generalized likelihood ratio test (GLRT), the adaptive linear-quadratic (ALQ), and the autoregressive generalized likelihood ratio (ARGLR) detectors by processing the real radar data. We show that the proposed detector offers a higher probability of detection than the other tests, for a given probability of false alarm.**

***Index Terms*—Detection, GARCH processes, GARCH-2D, non-Gaussian clutter, radar.**

I. Introduction

In radar applications it is important to properly model the contribution of the reflections on the environment to the measured signals in order to achieve a desired performance. These reflections on the environment, or clutter, are in many cases of nonhomogeneous nature and unknown statistics, requiring adaptive detection algorithms. Given its mathematical tractability, adaptive radar detection based on Gaussian clutter models has been extensively investigated [1]–[5]. A well known solution is the generalized likelihood ratio test (GLRT) [2] designed assuming a Gaussian clutter model with unknown covariance matrix. For this detection scheme two sets of input data are used which are called the primary and secondary inputs. The possibility of signal presence is accepted for the primary data while the secondary data are assumed to contain only clutter, independent of and identically distributed to the clutter components of the primary data. For the autoregressive generalized likelihood ratio (ARGLR) detector [4] the clutter is modeled by an autoregressive (AR) process to impose a structure on its covariance matrix. In this case the detector adjusts itself to the environment using only the primary data.

However, experimental evidence shows that the Gaussian assumption is not met in many situations of practical interest [6], [7]. Thus depending on the application, clutter models have been proposed based on distributions such as Log-normal, Weibull, K [8], [9], generalized compound probability density function [10]–[12] or on spherically invariant random process [13]. The detection problem for some of these non-Gaussian clutter models has also been studied [14]–[16]. The adaptive linear-quadratic (ALQ) detector [16] is a suboptimum approach designed assuming a compound-Gaussian clutter model. The problem formulation of this detector is analogous to the GLRT detector, and it also requires primary and secondary data sets.

Recently, a different approach to the adaptive detection problem was proposed considering a generalized autoregressive conditional heteroscedastic (GARCH) process to model the clutter [17]. GARCH processes [18] have heavy tailed probability density function (pdf) and volatility clustering, i.e., large changes tend to follow large changes and small changes tend to follow small ones, which is usually a desirable characteristic for clutter models. The resulting adaptive detector outperforms Gaussian and Weibull clutter model detectors in different practical situations. However, the GARCH detector in [17] has the disadvantage of not being able to incorporate information of several radar pulses in the decision rule since the GARCH process was used to model the clutter only in range (or fast time) dimension. Two dimensional GARCH processes (GARCH-2D) exist in the literature [19], [20], but they were never used to model radar clutter as far as we are aware of. Multidimensional GARCH processes have been used to model wavelet coefficients in anomalies detection in sonar applications [20] and in speckle suppression in synthetic aperture radar images [19].

In this work we extend our previous ideas, presented in [17], by proposing a clutter model that combines a GARCH-2D process with an AR process to use the information of multiple pulses in a decision, and we derive a detector suited for this clutter model. The GARCH-2D part of the model preserves the impulsivity property of the GARCH processes, i.e., it preserves

Manuscript received December 09, 2013; revised April 15, 2014; accepted June 13, 2014. Date of publication June 27, 2014; date of current version July 10, 2014. The associate editor coordinating the review of this manuscript and approving it for publication was Prof. Stefano Marano. This work was supported by the Agencia Nacional de Promoción Científica y Tecnológica (ANPCyT) PICT 2011-11-0909, the Universidad Nacional de La Plata (UNLP) 11-I-166, the Consejo Nacional de Investigaciones Científicas y Técnicas (CONICET) and the Comisión de Investigaciones Científicas de la provincia de Buenos Aires (CIC-PBA).

J. P. Pascual, N. von Ellenrieder, and M. Hurtado are with Laboratorio de Electrónica Industrial, Control e Instrumentación (LEICI), Universidad Nacional de La Plata, Buenos Aires, Argentina, and CONICET, C.A.B.A., Argentina (C1033AAJ) (e-mail: juanpablo.pascual@ing.unlp.edu.ar; ellenrie@ing.unlp.edu.ar; martin.hurtado@ing.unlp.edu.ar).

C. H. Muravchik is with LEICI, Universidad Nacional de La Plata, Buenos Aires, Argentina, and CIC-PBA, La Plata, Buenos Aires, Argentina (1900) (e-mail: carlosm@ing.unlp.edu.ar).

Color versions of one or more of the figures in this paper are available online at http://ieeexplore.ieee.org.

Digital Object Identifier 10.1109/TSP.2014.2332439

the heavy tailed pdf, and the AR model in the innovations lets us model pulsewise correlation. We develop an adaptive detection algorithm based on this AR-GARCH-2D clutter model. We carry out a theoretical analysis to determine its false alarm probability. By means of numerical simulations we compute the detection probability to evaluate the AR-GARCH-2D detector performance. We also analyze how the estimation error of its parameters affects the performance. Although the resulting detector is not constant false alarm rate (CFAR) with respect to the process coefficients, we show that it is very robust in practical situations, i.e., the probability of false alarm does not significantly change when the coefficient values vary. We test AR-GARCH-2D detectors with different model orders in a real situation using sea data measurements and we apply a model selection criteria to choose the AR-GARCH-2D model that best fits the data. Finally, we compare the performance of our method with the GLRT [2], the ALQ [16] and the ARGLR [4] detectors using the sea data measurements.

Notation

We adopt the following notation. We use math italic for scalars x, uppercase bold for matrices $\mathbf{X}$ and lowercase bold for vectors $\mathbf{x}$. For a matrix $\mathbf{X}$ the vectors $\mathbf{x}_j$ and $\mathbf{x}^i$ represent the j^{th} column and the i^{th} row respectively, and the scalar x_{ij} is the ij^{th} entry of the matrix $\mathbf{X}$. In addition, $\{x_j\}_{j=1}^{M}$ represents the set of M scalars $x_1, x_2, \ldots, x_M$.

For random variables x, y and z, the variable $x/(y;z)$ denotes the conditional random varible x given y and z.

The expectation and variance operators are denoted as $\mathbb{E}\{\cdot\}$ and $\mathbb{V}\{\cdot\}$ respectively.

II. Clutter Model

A. AR-GARCH-2D Process

Let the doubly indexed process v_{rt} represent a 2D stochastic process that models the clutter. The first index, r, corresponds to the range (or fast time) dimension and the second index, t, corresponds to the pulse (or slow time) dimension. Then, based on a GARCH-2D process [19] we define a complex AR-GARCH-2D process, v_{rt}, as

$$v_{rt} = \sigma_{rt} z_{rt} + \sum_{j=1}^{M} a_{0j} v_{r,t-j}, \quad z_{rt} \sim \mathcal{CN}(0,1) \text{ i.i.d.}, \quad (1)$$

$$\sigma_{rt}^2 = k + \sum_{i,j \in \wedge_1} \alpha_{ij} \sigma_{r-i,t-j}^2 + \sum_{i,j \in \wedge_2} \beta_{ij} |v_{r-i,t-j}|^2, \quad (2)$$

where $\mathcal{CN}$ denotes a circularly-symmetric normal distribution, a_{0j} are the coefficients of the autoregressive part of the process, σ_{rt}^2 is the conditional variance, given by (2), with k being the independent term that sets a variance floor, α_{ij} the coefficients of the autoregressive part of the conditional variance, and β_{ij} the coefficients involving the squared past returns. To ensure that the conditional variance, σ_{rt}^2, is always positive we must impose the following constraints

$$k > 0 \quad \alpha_{ij} \geqslant 0,\ (i,j) \in \wedge_1 \quad \beta_{ij} \geqslant 0,\ (i,j) \in \wedge_2. \quad (3)$$

Let also

$$\wedge_1 = \{(i,j)/0 \leqslant i \leqslant p_1, 0 \leqslant j \leqslant p_2, (i,j) \neq (0,0)\}, \quad (4)$$

$$\wedge_2 = \{(i,j)/0 \leqslant i \leqslant q_1, 0 \leqslant j \leqslant q_2, (i,j) \neq (0,0)\}, \quad (5)$$

where p_1, p_2, q_1 and q_2 are the process orders. The AR-GARCH-2D process defined above differs from the GARCH-2D process proposed in [19] only by the inclusion of the second term on the right hand side of (1), i.e., the term of the autoregressive part in the second (slow) time index. Thus, while the GARCH-2D process is serially uncorrelated, the AR-GARCH-2D process lets us model the pulsewise correlation while preserving the impulsivity property of the GARCH processes. It models the returns as correlated Gaussian noise processes with nonconstant conditional variance (1). For every location (r,t), both the neighborhood of the return process and the neighborhood of the conditional variance play a role in the current conditional variance (2), which leads to clustering of variations. In this model the number of conditional variance coefficients increases drastically with the orders p_1, p_2, q_1 and q_2, which severely hinders an accurate estimation of the process coefficients. To make the model tractable for applied purposes, additional structure may be imposed. Since for a GARCH-1D model, a GARCH process with only two coefficients, k and the first β, is enough to capture much of the statistical behavior of sea clutter [17] we restrict our analysis to the model

$$v_{rt} = \sigma_{rt} z_{rt} + \sum_{j=1}^{M} a_{0j} v_{r,t-j}, \quad z_{rt} \sim \mathcal{CN}(0,1) \text{ i.i.d.}, \quad (6)$$

$$\sigma_{rt}^2 = k + \sum_{j=0}^{1} \alpha_{1j} \sigma_{r-1,t-j}^2 + \sum_{j=0}^{1} \beta_{1j} |v_{r-1,t-j}|^2, \quad (7)$$

where the coefficients α_{01} and β_{01} were excluded in order to obtain a closed form expression for the detector that we deduce in Section III. The coefficients α impose some smoothness on σ_{rt} and coefficients β determine the degree of dependence with previous outputs. By restricting this dependence to the previous range cell and pulse, we capture only the dominant dynamics of the conditional variance. More complex dynamics could be modeled with higher orders. Most clutter environments are probably modeled adequately by this closest neighbors dependence, but even if some environments exhibit more complex clutter dynamics, a model with extra coefficients does not imply a better fit in practice, since a higher number of coefficients would lead to higher estimation errors for a given dataset. Furthermore, we restrict M to vary only from 0 to 3 because an AR clutter model of third order was found to be a good compromise between model fidelity and mathematical tractability [21].

Let $\psi_{r-1,t}$ denote the set of all information up to range cell $r-1$ and time t, i.e., $\sigma_{\rho\tau}^2$ and $v_{\rho\tau}$ for $\rho \leqslant r-1$ and $\tau \leqslant t$. Then, if we condition v_{rt} to $\left(\psi_{r-1,t}; \{v_{r,t-j}\}_{j=1}^{M}\right)$ from (6) we see that σ_{rt} and $\sum_{j=1}^{M} a_{0j} v_{r,t-j}$ are given and only $z_{rt} \sim \mathcal{CN}(0,1)$ is random, thus

$$v_{rt} / \left(\psi_{r-1,t}; \{v_{r,t-j}\}_{j=1}^{M}\right) \sim \mathcal{CN}\left(\sum_{j=1}^{M} a_{0j} v_{r,t-j}; \sigma_{rt}^2\right). \quad (8)$$

Note that the set of process samples $\{v_{r,t-j}\}_{j=1}^{M}$ is not included in $\psi_{r-1,t}$.

Since the model involves autoregressive equations it could diverge. To avoid this situation it is possible to impose conditions on the process coefficients in order to ensure that the process is wide sense stationary and with finite variance, as in GARCH-1D processes [18] or GARCH-2D processes [20]. It is possible to show that $\mathbb{E}\{v_{rt}\} = 0$ and the unconditional variance is finite and equal to

$$\mathbb{V}\{v_{rt}\} = \frac{k}{1-\sum_{j=0}^{1}\alpha_{1j}-\sum_{j=0}^{1}\beta_{1j}-\left(1-\sum_{j=0}^{1}\alpha_{1j}\right)\phi_M}, \quad (9)$$

as long as the condition

$$\sum_{j=0}^{1}\alpha_{1j}+\sum_{j=0}^{1}\beta_{1j}+\left(1-\sum_{j=0}^{1}\alpha_{1j}\right)\phi_M < 1, \quad (10)$$

is satisfied, where ϕ_M is a constant that depends on the a_{0j} coefficients. In Appendix A we present the expression of ϕ_M for $M = 0$ to 3. As in the case of the GARCH-1D and GARCH-2D processes, there is no explicit expression for the probability density function of the AR-GARCH-2D process.

B. Parameter Estimation

To fit the AR-GARCH-2D model to the clutter we should estimate its coefficients from a target-free dataset. Assuming a single sensor pulsed radar transmits a coherent train of T pulses and the receiver samples the reflected signal from each pulse at the output of the matched filter to form R range cells. The samples of the complex envelope at the output of the quadrature demodulator can be assembled into a matrix $\mathbf{V} \in \mathbb{C}^{R\times T}$ with complex elements $[\mathbf{V}]_{rt} = v_{rt}$, the rows corresponding to the range dimension and columns corresponding to the pulse dimension.

A possible way to perform the estimation would be using the maximum likelihood (ML) method, but there is no explicit expression for the pdf of an AR-GARCH-2D process. To overcome this difficulty, analogously to the case of the GARCH-1D [18] or GARCH-2D [20] processes, we consider instead the conditional likelihood function $f(\mathbf{V}/\psi_{R-1,-M};\psi_{0T};\mathbf{v}_{1-M};\cdots;\mathbf{v}_0)$ that may be written as

$$f(\mathbf{V}/\psi_{R-1,-M};\psi_{0T};\mathbf{v}_{1-M};\cdots;\mathbf{v}_0) = \prod_{r=1}^{R}\prod_{t=1}^{T} f(v_{rt}/\psi_{r-1,t};\{v_{t-j}\}_{j=1}^{M}), \quad (11)$$

where $\mathbf{v}_t = [v_{1t}\ v_{2t}\ \cdots\ v_{Rt}]^T$ and the conditional pdfs $f(v_{rt}/\psi_{r-1,t};\{v_{t-j}\}_{j=1}^{M})$ are given by (8). Then, we define the function $\ell(\boldsymbol{\theta})$ as

$$\ell(\boldsymbol{\theta}) = \sum_{r=1}^{R}\sum_{t=1}^{T}\left[\ln(\sigma_{rt}^2)+\frac{1}{\sigma_{rt}^2}\left|v_{rt}-\sum_{j=1}^{M}a_{0j}v_{r,t-j}\right|^2\right], \quad (12)$$

where $\boldsymbol{\theta} = [k\ \alpha_{10}\ \alpha_{11}\ \beta_{10}\ \beta_{11}\ a_{01}\ \cdots\ a_{0M}]^T$ is the parameter vector that we want to estimate. The conditional log-likelihood function $-\ln(f(\mathbf{V}/\psi_{R-1,-M};\psi_{0T};\mathbf{v}_{1-M};\cdots;\mathbf{v}_0))$ differs from $\ell(\boldsymbol{\theta})$ in a constant.

Finally, the quasi-maximum likelihood estimator (QMLE), $\hat{\boldsymbol{\theta}}$, is the value of $\boldsymbol{\theta}$ that maximizes (11) or, equivalently, that minimizes $\ell(\boldsymbol{\theta})$ subject to the constraints given by (3) and (10). In summary, we may write

$$\hat{\boldsymbol{\theta}} = \underset{\boldsymbol{\theta}\in\Theta}{\operatorname{argmin}}\,\ell(\boldsymbol{\theta}), \quad (13)$$

where Θ is the set of values of $\boldsymbol{\theta}$ that satisfy the constraints (3) and (10). Note that the QMLE is not an approximation of the ML estimator, it is simply a different estimator.

III. Detection

For a given range cell r, N complex samples from the pulse dimension $\{y_{rt}\}_{t=1}^{N}$ can be assembled into an N-dimentional vector $\mathbf{y}^r = [y_{r1}\ y_{r2}\ \cdots\ y_{rN}]^T$. Then, the detection procedure is given by a binary hypothesis test between hypotheses H_0 and H_1 once $\mathbf{y}^r$ has been measured from the range cell under test

$$\begin{aligned} H_0 &: \mathbf{y}^r = \mathbf{v}^r \\ H_1 &: \mathbf{y}^r = \mathbf{s}^r + \mathbf{v}^r. \end{aligned} \quad (14)$$

Under the null hypothesis H_0, it is assumed that the measurements consist only of clutter $\mathbf{v}^r$. We assume that the electronic noise is negligible or part of the clutter model. Under the hypothesis H_1, it is assumed that the measurements are the combined result of clutter and echoes from a target, $\mathbf{s}^r$. We model the signal vector in the form $\mathbf{s}^r = \gamma\mathbf{p}^r$, where γ is an deterministic but unknown complex scalar, while $\mathbf{p}^r$ is a perfectly known complex vector whose elements are given by $[\mathbf{p}^r]_t = p_{rt} = e^{j\Omega t}$, with $\Omega = 2\pi f_d T_s$ where f_d is the target Doppler frequency and T_s is the radar pulse repetition interval [16]. We assume that the statistics of the clutter is the same for both hypotheses and it is modeled as an AR-GARCH-2D process.

The generalized likelihood ratio test (GLRT) involves the ratio of the likelihood functions under each hypotheses, evaluated at their respective maxima -given by the MLEs of all unknown parameters corresponding to each hypotheses [22]. Since no explicit expression exists for the distribution of an AR-GARCH-2D process, there is also no expression for the likelihood ratio to obtain the decision rule. Thus, the classical GLRT approach can not be used in our case. Instead, we develop our test based on the conditional likelihood functions given the process observations up to the range cell under test [17]. This generalized conditional likelihood ratio test makes use of the information available up to the moment of the test to define the hypotheses, and seems a good alternative to the classic GLRT in which the hypotheses are based on the model but are not updated by previous observations.

The conditional pdfs are given by

$$f_i(\mathbf{y}^r/\psi_{r-1,N};\{y_{r,t-M}\}_{t=1}^{M}) = \prod_{t=1}^{N} f_i(y_{rt}/\psi_{r-1,t};\{y_{r,t-j}\}_{j=1}^{M}), \quad (15)$$

with $i = 0, 1$. Under the clutter-alone hypothesis, from (8) we get

$$f_0(y_{rt}/\psi_{r-1,t}; \{y_{r,t-j}\}_{j=1}^{M}) = \frac{1}{\pi\sigma_{rt}^2} e^{\frac{-1}{\sigma_{rt}^2}\left| y_{rt} - \sum_{j=1}^{M} a_{0j} y_{r,t-j} \right|^2}. \tag{16}$$

Under the signal-plus-noise hypothesis, the elements of $\mathbf{y}^r$ may be written as $y_{rt} = \gamma p_{rt} + v_{rt}$ and from (6) it results

$$y_{rt} = \gamma p_{rt} + \sum_{j=1}^{M} a_{0j} v_{r,t-j} + \sigma_{rt} z_{rt}. \tag{17}$$

Writing the clutter samples as $v_{r,t-j} = y_{r,t-j} - \gamma p_{r,t-j}$ for $j = 1, \ldots, M$, from (17), we find

$$y_{rt} = \sum_{j=1}^{M} a_{0j} y_{r,t-j} + \gamma \left(p_{rt} - \sum_{j=1}^{M} a_{0j} p_{r,t-j} \right) + \sigma_{rt} z_{rt}. \tag{18}$$

Hence, $f_1(y_{rt}/\psi_{r-1,t}; \{y_{r,t-j}\}_{j=1}^{M})$ is also a normal pdf but with a different mean value

$$f_1(y_{rt}/\psi_{r-1,t}; \{y_{r,t-j}\}_{j=1}^{M}) = \frac{1}{\pi\sigma_{rt}^2} e^{\frac{-1}{\sigma_{rt}^2}\left| y_{rt} - \sum_{j=1}^{M} a_{0j} y_{r,t-j} - \gamma\left(p_{rt} - \sum_{j=1}^{M} a_{0j} p_{r,t-j} \right) \right|^2}. \tag{19}$$

Following the GLRT approach we should maximize $f_i(\mathbf{y}^r/\psi_{r-1,N}; \{y_{r,t-M}\}_{t=1}^{M})$ with respect to the unknown parameters $\boldsymbol{\theta}$ and γ, separately for each $i = 0, 1$. However, the application of the GLRT methodology for the AR-GARCH-2D coefficients would lead to a multidimensional nonlinear maximization problem for which no closed form solution exists. We propose an alternative solution based on the assumption that the value of the coefficients of the AR-GARCH-2D process is known. Then, in the algorithm implementation we will estimate them as explained in Section II-B, making use of a clutter-only secondary data set.

Under this assumption the only unknown parameter is γ, and it only appears in the pdf of the hypothesis H_1. Then, as shown in Appendix B

$$\hat{\gamma} = \frac{\sum_{t=1}^{N} \frac{1}{\sigma_{rt}^2} \left(p_{rt} - \sum_{j=1}^{M} a_{0j} p_{r,t-j} \right)^* \left(y_{rt} - \sum_{j=1}^{M} a_{0j} y_{r,t-j} \right)}{\sum_{t=1}^{N} \frac{1}{\sigma_{rt}^2} \left| p_{rt} - \sum_{j=1}^{M} a_{0j} p_{r,t-j} \right|^2}, \tag{20}$$

is the value of γ that maximizes $f_1(\mathbf{y}^r/\psi_{r-1,N}; \{y_{r,t-M}\}_{t=1}^{M})$.

Then, we use the conditional likelihood ratio, $\Lambda(\mathbf{y}^r)$, and we establish the following decision rule

$$\Lambda(\mathbf{y}^r) = \frac{f_1(\mathbf{y}^r, \hat{\gamma}/\psi_{r-1,N}; \{y_{r,t-M}\}_{t=1}^{M})}{f_0(\mathbf{y}^r/\psi_{r-1,N}; \{y_{r,t-M}\}_{t=1}^{M})} \underset{H_0}{\overset{H_1}{\gtrless}} \lambda, \tag{21}$$

where λ is the decision threshold to be determined. Replacing the expressions of the pdfs and $\hat{\gamma}$ in (21), it is possible to rewrite the decision rule as

$$\left| \sum_{t=1}^{N} \frac{1}{\sigma_{rt}^2} \left(p_{rt} - \sum_{j=1}^{M} a_{0j} p_{r,t-j} \right)^* \left(y_{rt} - \sum_{j=1}^{M} a_{0j} y_{r,t-j} \right) \right| \underset{H_0}{\overset{H_1}{\gtrless}} \eta, \tag{22}$$

where the threshold η is given by

$$\eta = \sqrt{\lambda \sum_{t=1}^{N} \frac{1}{\sigma_{rt}^2} \left| p_{rt} - \sum_{j=1}^{M} a_{0j} p_{r,t-j} \right|^2}. \tag{23}$$

In the classic approach, the next step would be to obtain an expression of the false alarm probability, P_{FA}, in terms of the threshold, η or λ, and then invert it to obtain the threshold setting in terms of P_{FA}. This procedure requires knowing the distribution of the statistic on (22) under the hypothesis H_0. Again, we do not have an explicit expression of the pdf of v_{rt} or y_{rt}. Hence, to determine a threshold we resort to the conditional false alarm probability given $\psi_{r-1,N}$, i.e., $P_{FA}/\psi_{r-1,N}$. Taking into account that under the hypothesis H_0 $y_{rt} = v_{rt}$, then

$$y_{rt} - \sum_{j=1}^{M} a_{0j} y_{r,t-j} = v_{rt} - \sum_{j=1}^{M} a_{0j} v_{r,t-j} = \sigma_{rt} z_{rt}, \tag{24}$$

and under these conditions, the statistic reduces to

$$\left| \sum_{t=1}^{N} \frac{1}{\sigma_{rt}} \left(p_{rt} - \sum_{j=1}^{M} a_{0j} p_{r,t-j} \right)^* z_{rt} \right| = \left| \sum_{t=1}^{N} w_{rt} \right|, \tag{25}$$

where

$$w_{rt}/\psi_{r-1,N} \sim \mathcal{CN}\left(0; \frac{1}{\sigma_{rt}^2} \left| p_{rt} - \sum_{j=1}^{M} a_{0j} p_{r,t-j} \right|^2 \right). \tag{26}$$

If we define $S_r = \sum_{t=1}^{N} w_{rt}$ and $\Gamma = |S_r|$, then $S_r/\psi_{r-1,N}$ is the sum of N independent complex normal random variables. Thus, from (26)$S_r/\psi_{r-1,N} \sim \mathcal{CN}(0, \sigma_s^2)$, with

$$\sigma_s^2 = \sum_{t=1}^{N} \frac{1}{\sigma_{rt}^2} \left| p_{rt} - \sum_{j=1}^{M} a_{0j} p_{r,t-j} \right|^2. \tag{27}$$

Hence, $\Gamma/\psi_{r-1,N}$ is Rayleigh distributed and $P_{FA}/\psi_{r-1,N}$ is given by

$$P_{FA}/\psi_{r-1,N} = \int_{\eta}^{\infty} f_{\Gamma}(\Gamma/\psi_{r-1,N}; H_0) d\Gamma = e^{-\eta^2/\sigma_s^2}. \tag{28}$$

Finally, from (23) and (28) we obtain the threshold λ

$$\lambda = -\ln(P_{FA}/\psi_{r-1,N}). \tag{29}$$

The probability of detection, P_D, cannot be evaluated analytically and it will be computed in Sections IV-B and V by means of Monte Carlo simulations using synthetic and real clutter data, respectively.

In the derivation of the decision algorithm we assume the process coefficients are known, however it is not true in a real situation. Thus, in practice the AR-GARCH-2D detector is given by

$$\frac{\left|\sum_{t=1}^{N}\frac{1}{\hat{\sigma}_{rt}^2}\left(p_{rt}-\sum_{j=1}^{M}\hat{a}_{0j}p_{r,t-j}\right)^{*}\left(y_{rt}-\sum_{j=1}^{M}\hat{a}_{0j}y_{r,t-j}\right)\right|^2}{\sum_{t=1}^{N}\frac{1}{\hat{\sigma}_{rt}^2}\left|p_{rt}-\sum_{j=1}^{M}\hat{a}_{0j}p_{r,t-j}\right|^2}\underset{H_0}{\overset{H_1}{\gtrless}}\lambda, \tag{30}$$

where

$$\hat{\sigma}_{rt}^2=\hat{k}+\sum_{j=0}^{1}\hat{\alpha}_{1j}\hat{\sigma}_{r-1,t-j}^2+\sum_{j=0}^{1}\hat{\beta}_{1j}|y_{r-1,t-j}|^2, \tag{31}$$

and $\hat{k}$, $\hat{\alpha}_{1j}$, $\hat{\beta}_{1j}$, for $j=0,1$ and $\hat{a}_{0j}$, for $j=1,\ldots,M$ are the estimates of the process coefficients. In Section IV-C we perform a sensibility analysis to analyze how errors in the coefficient values affect the performance.

IV. Numerical Simulations

In this section we carry out a numerical analysis of the estimation method of the AR-GARCH-2D process coefficients and of the detection performance of the AR-GARCH-2D detector. For the numerical simulations, we restrict our analysis to one of the processes of the family represented by AR-GARCH-2D model. Synthetic data used in this section is generated by means of the following model

$$\begin{aligned}v_{rt}&=(1.049-j1.079)v_{r,t-1}+(0.097+j0.441)v_{r,t-2}\\&\quad+(0.063+j0.151)v_{r,t-3}+\hat{\sigma}_{rt}z_{rt},\end{aligned} \tag{32}$$

$$\hat{\sigma}_{rt}^2=1.244\times10^{-4}+0.022\sigma_{r-1,t-1}^2+0.012|v_{r-1,t}|^2, \tag{33}$$

with $z_{rt}\sim\mathcal{CN}(0,1)$ and i.i.d.. As we will show in Section V-A, this is the model obtained from the real clutter data fit.

A. Estimation

In order to verify that the estimates of the process coefficients satisfy desired properties and to have also a guideline to the estimation quality when real data are used, we performed an analysis of the estimation quality as a function of the number of samples of the observation matrix $\mathbf{V}$. This analysis was done by means of numerical simulations which consisted in the generation of independent process realizations of different size, $R\times T$, and the estimation of the model coefficients for each realization. The estimation problem given by (13), was solved using the Matlab *Active Set Algorithm*, implemented through the method SQP (*Sequential Quadratic Programming*) [23]. This procedure was repeated 200 times for each case, i.e., we obtained 200 values of the coefficient estimates for each synthetic dataset size. The initial conditions were chosen randomly within the set of coefficient values that satisfy the constraints (3) and (10). We did not prove the convexity of the problem, but the algorithm converged for all the tested initial values.

Tables I and II show mean and standard deviation values of the estimates as a function of the dataset size, $R\times T$. The mean of the estimates shows a small bias that decreases with the increase of the number of samples used in the estimation procedure. It can be seen that some coefficients are more sensitive to a dimension than the other, for example the bias of the estimator of α_{11} decreases rapidly for an increasing number of time samples but not of range samples. The standard deviation of the estimates decreases with the number of samples, as seen in Table II. Note that the results verify the mentioned asymptotic behavior with a rate of convergence close to the square root of the number of samples. In these examples, we see that the QMLE resembles the behavior of an asymptotically unbiased consistent estimator.

TABLE I
Mean of the Coefficient Estimates

Coef.	$R\times T$				
	68×2048	68×4096	136×2048	68×8192	136×4096
k	1.137×10^{-4}	1.202×10^{-4}	1.060×10^{-4}	1.240×10^{-4}	1.140×10^{-4}
α_{11}	0.093	0.052	0.140	0.029	0.089
β_{10}	0.012	0.012	0.011	0.012	0.012
a_{01}	$1.042-j1.068$	$1.045-j1.072$	$1.044-j1.070$	$1.046-j1.074$	$1.046-j1.073$
a_{02}	$0.092+j0.419$	$0.094+j0.427$	$0.093+j0.424$	$0.095+j0.433$	$0.094+j0.430$
a_{03}	$0.072+j0.156$	$0.069+j0.154$	$0.070+j0.155$	$0.067+j0.153$	$0.068+j0.153$

TABLE II
Standard Deviation of the Coefficient Estimates

Coef.	$R\times T$				
	68×2048	68×4096	136×2048	68×8192	136×4096
k	1.049×10^{-6}	6.185×10^{-7}	7.215×10^{-7}	4.211×10^{-7}	5.190×10^{-7}
α_{11}	4.901×10^{-3}	2.821×10^{-3}	3.820×10^{-3}	1.494×10^{-3}	3.027×10^{-3}
β_{10}	1.501×10^{-4}	1.097×10^{-4}	9.275×10^{-5}	8.453×10^{-5}	7.370×10^{-5}
a_{01}	2.611×10^{-3}	1.859×10^{-3}	1.961×10^{-3}	1.262×10^{-3}	1.422×10^{-3}
a_{02}	4.421×10^{-3}	3.209×10^{-3}	3.679×10^{-3}	2.251×10^{-3}	2.699×10^{-3}
a_{03}	2.460×10^{-3}	1.822×10^{-3}	2.147×10^{-3}	1.313×10^{-3}	1.597×10^{-3}

B. Probability of Detection

In order to evaluate the performance of the AR-GARCH-2D detector Monte Carlo simulations were performed to estimate the probability of detection, P_D, for different values of signal to clutter ratio (SCR). We generated realizations of an AR-GARCH-2D process given by (32) and (33) and added a synthetic target with the model proposed in Section III in a range cell chosen at random. The signal follows the Swerling I target model [24], i.e., γ is a complex circularly-symmetric normal random variable, with zero mean and variance $\mathbb{E}\{|\gamma|^2\}=\sigma_\gamma^2$, taking a different value in each decision. We defined $SCR=\sigma_\gamma^2/\hat{\sigma}^2$, where $\hat{\sigma}^2$ is the sample variance of the clutter data. We set the target Doppler frequency f_d such that $f_dT_s=0.5$ and selected the threshold λ from (29) to get a $P_{FA}=10^{-2}$ and $P_{FA}=10^{-3}$. For each value of P_{FA} we repeated the procedure for $N=4,8$ and 16 pulses. We estimated P_D by the relative frequency of the statistic exceeding the threshold.

We generated synthetic datasets of size 68×8192 (equal to the size of the real radar datasets used in Section V) and we used a number of independent datasets large enough to ensure that the detection probability is accurately estimated [22]. We repeated

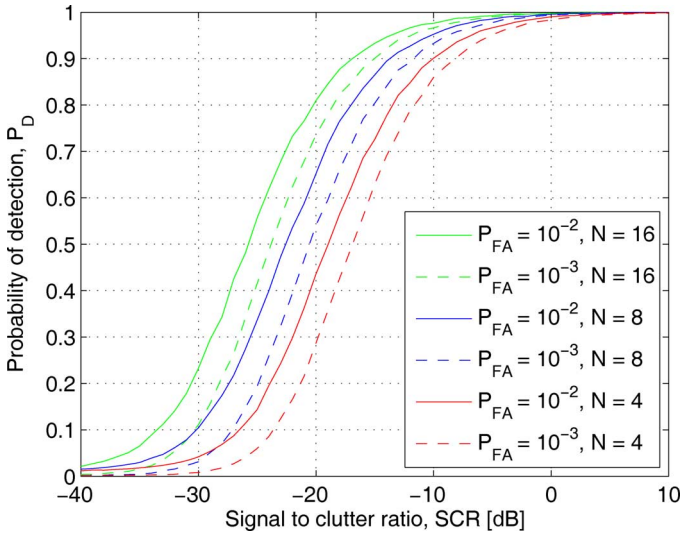

Fig. 1. Probability of detection versus signal to clutter ratio for the AR-GARCH-2D detector using synthetic data.

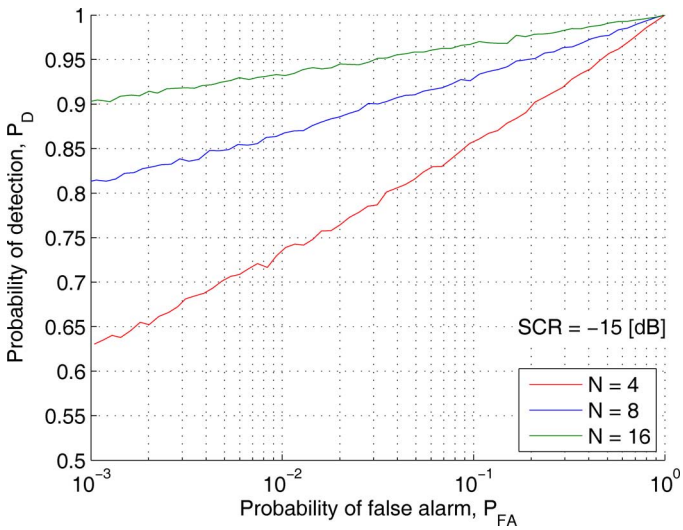

Fig. 2. Empirical ROC curves for the AR-GARCH-2D detectors using synthetic data.

the simulations for different values of SCR, keeping the noise power constant and varying the value of σ_γ^2. Fig. 1 shows the estimated P_D values obtained by numerical simulations. As expected for a given value of SCR the detection probability increases with P_{FA} and N.

Finally, we computed the receiver operating characteristic (ROC) curve for the AR-GARCH-2D detector. A pair (P_{FA}, P_D) corresponds to a point on the curve. For a given SCR the ROC was obtained by varying the threshold and computing the false alarm probability using (29) and the detection probability by means of its relative frequency. Fig. 2 shows ROC curves for $N = 4, 8,$ and, 16 with $SCR = -15$ dB.

C. Sensitivity Analysis

In the derivation of the AR-GARCH-2D detector we assume that the process coefficients are known. However, in a real situation this is seldom true and they have to be estimated. Thus, in this section we evaluate how the variance of the coefficient estimates affect the performance of the detector. In the presence of an estimation error or small changes in the parameters the performance of the detector should not vary.

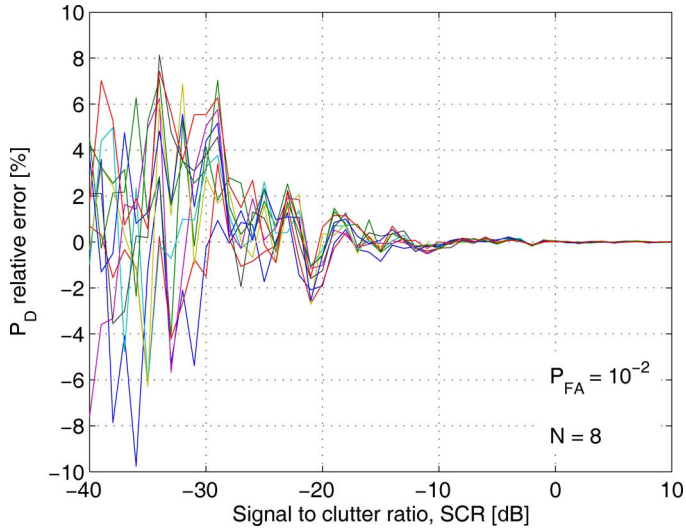

Fig. 3. Effect of the coefficient estimation errors on the probability of detection of the AR-GARCH-2D detector.

We performed simulations generating the clutter with the true coefficient values and we computed the P_D and the P_{FA}, assuming that in the detector the coefficients were corrupted due to estimation errors. We draw random coefficient values from a normal distribution with mean and standard deviations obtained for coefficient estimates in Section IV-A (Tables I and II) for the synthetic datasets of size 68×8192.

To estimate the probability of detection the procedure was the same as described in the previous section, with $N = 8$ and λ set to get $P_{FA} = 10^{-2}$. The simulation was repeated 10 times, i.e., for ten different sets of corrupted coefficient values. Fig. 3 shows the relative error of the P_D obtained for different values of SCR, where the P_D obtained in Section IV-B was taken as the true value. We observe that the detector presents a low error in P_D for a wide range of SCR values, and it becomes negligible for high SCR.

To estimate the probability of false alarm the approach was similar. In this case the target was not added to the clutter data. The statistic was computed with the corrupted coefficients and compared to the threshold, and the P_{FA} was estimated by its relative frequency. This procedure was repeated varying the threshold, λ, to get a curve P_{FA} as a function of λ.

A desirable feature for a radar detector is to have a constant false alarm rate (CFAR), i.e., the dispersion of the unknown parameters should not affect the false alarm probability. Thus, in the presence of an estimation error or small variations in the parameters, the performance of the detector should not vary. Fig. 4 shows ten curves of P_{FA} obtained from random coefficients and the theoretical conditional P_{FA}, given by (29), as a function of λ. We can see that even though the AR-GARCH-2D detector is not CFAR with respect to the process coefficients from an analytical point of view, it is very robust in practical situations, i.e., P_{FA} does not significantly change when the coefficient values change.

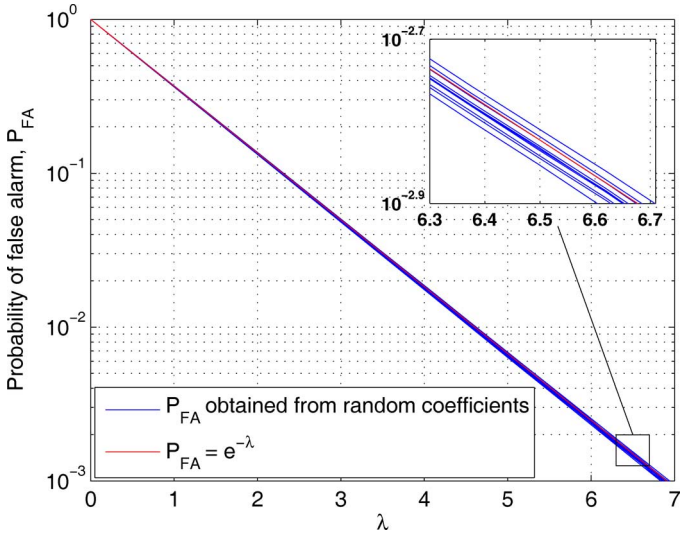

Fig. 4. Effect of the coefficient estimation errors on the probability of false alarm of the AR-GARCH-2D detector.

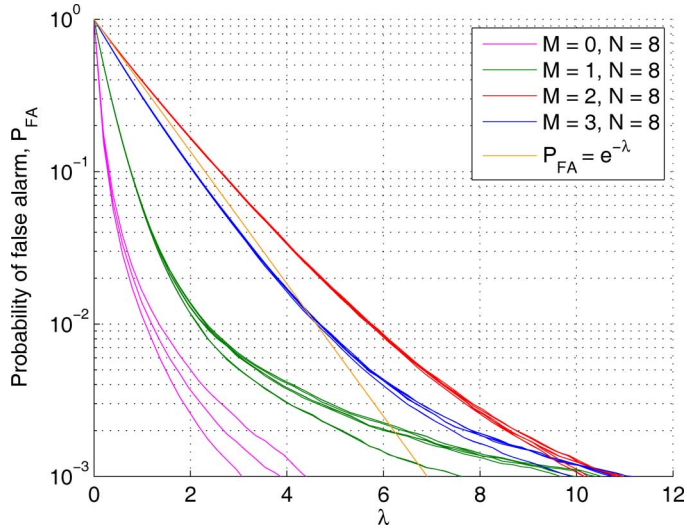

Fig. 5. Probability of false alarm versus threshold for the AR-GARCH-2D detectors using IPIX radar clutter data.

V. Performance Analysis

In this section the AR-GARCH-2D detector is tested on real sea clutter data to evaluate its performance in a real application situation. We use data from the McMaster University IPIX radar, collected at the Osborne Head Gunnery Range (OHGR), Dartmouth, Nova Scotia, Canada [6]. Specifically, we use the data recorded on November 10, 1993 at 00:34:24 a.m., at 00:36:51 a.m. and at 00:39:10 a.m. in the data sets *stare6*, *stare7* and *stare8* respectively. The IPIX radar has polarimetric information, shown results correspond to vertical polarization (VV) only. The datasets correspond to inhomogeneous sea clutter without a target. The height of the sea waves was of approximately 0.9 m. For the three data sets the fast time or range dimension consists of $R = 68$ samples, the sampling interval is 15 m and the radar range resolution is 30 m. The number of transmitted pulses, i.e., the number of samples in the slow time dimension, is $T = 8192$ with a pulse repetition frequency of 500 Hz.

A. Model Fit to the Clutter Data

To model the clutter as an AR-GARCH-2D process, we are interested in fitting the AR-GARCH-2D process to the samples from clutter measurements. The fit includes the estimation of the coefficients of the process as well as the selection of the process order, i.e., the optimum number of coefficients. To carry out the fit we use only the data set *stare6*; the rest of the data sets will be used to evaluate the performance of the detection algorithm. The coefficients estimation was performed using the methodology described in Section IV-A for the numerical simulations. Since the orders of the process, i.e., the number of coefficients, are not known a priori, the estimation of the coefficients was repeated for different orders. For each value of M between 0 and 3 we considered all possible combinations of variance coefficients assuming that they can be zero or nonzero. Taking into account that for a GARCH model β's coefficients can not be all simultaneously zero, we have 48 possible models. However, when we performed the fit for some model orders the estimates corresponding to some coefficients took the same values as in the case of other AR-GARCH-2D process fit, and the estimates of the new coefficients did not appear to be statistically significant. Eliminating such cases, the number of survivors models reduces to 27; 8 correspond to models for which $M = 1, 2, 3$ and the remaining 3 correspond to $M = 0$.

A fair comparison among the proposed models should not be made based only on the quality of the fit of the probability distributions, but also on a comparison of the performance of the detection problem. Thus, before adopting a model selection criteria to determine the model with optimum compromise between model complexity and fit to the clutter measurements, we carry out a performance analysis of the detection problem for all the AR-GARCH-2D models.

To evaluate the performance of the detectors given by (30) we use the data sets *stare7* and *stare8* that have not been used in the estimation procedure, with $N = 8$ pulses. We computed the P_{FA} and the P_D in the same way as described in Section IV but using real clutter data instead of the synthetic clutter.

Fig. 5 shows the curves of the empirical probability of false alarm, P_{FA}, for the different AR-GARCH-2D detectors, corresponding to the 27 models obtained from the fit, and the theoretical conditional P_{FA}, given by (29), as a function of the threshold λ. We define the empirical false alarm rate as the number of decisions exceeding the threshold divided by the total number of decisions $2RT/N$. We use the value of M to group the models because, as can be seen in the figure, the processes with equal autoregressive order present a similar behavior. Note that processes for which $M = 3$ approximate better the probability of false alarm than the others models.

In order to evaluate the probability of detection P_D we added a synthetic target with the model described in Section IV-B to the real sea clutter data. Again, we defined $SCR = \sigma_\gamma^2/\hat{\sigma}^2$, where now $\hat{\sigma}^2$ is the sample variance of the real clutter data. We selected the threshold λ for each detector to get a $P_{FA} = 10^{-2}$, based on the results of Fig. 5. Fig. 6 shows the curves of the empirical P_D for the different AR-GARCH-2D detectors as a function of the SCR. The empirical detection rate is defined as

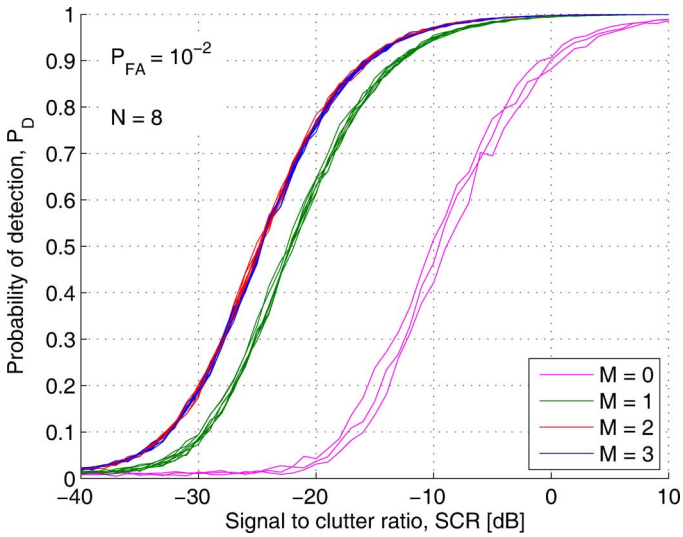

Fig. 6. Probability of detection versus signal to clutter ratio for the AR-GARCH-2D detectors using IPIX radar clutter data and a synthetic target.

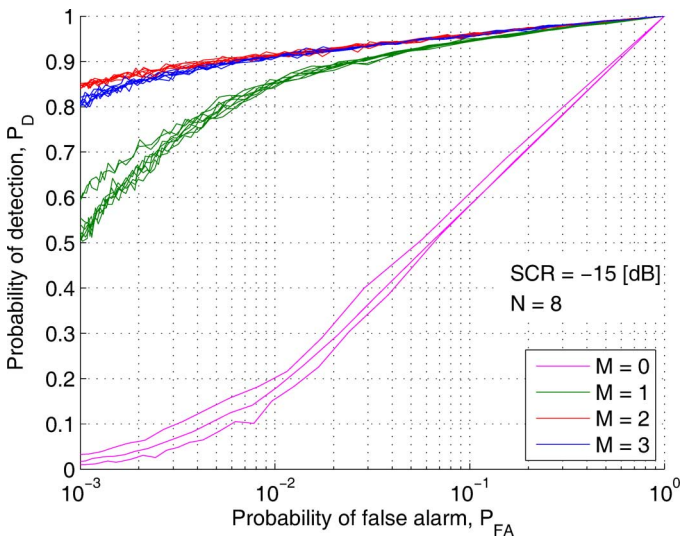

Fig. 7. Empirical ROC curves for the AR-GARCH-2D detectors using IPIX radar clutter data and a synthetic target.

the number of detections in the range cell where the target is located divided by the total number of decisions in this range cell. This was repeated for 16 different range cells taken randomly from either of the two datasets, yielding a total number of $16T/N$ decisions. The results show that the performance of the processes with orders $M = 2$ and $M = 3$ is similar and it is better than the performance of the remaining models.

Finally, we compute the receiver operating characteristic (ROC) curve for the AR-GARCH-2D detectors. In this case the ROC was obtained using the real clutter data, by varying the threshold and computing the empirical detection and false alarm rates. Fig. 7 shows the empirical ROC curves for actual clutter data and a synthetic target with $SCR = -15$ dB. Again we observe better results for models with second and third autoregressive order.

To evaluate which AR-GARCH-2D models show a better compromise between model complexity and quality of fit we use the Bayesian information criterion (BIC) [25]. Ignoring a constant term shared by all the models, from (12) the BIC statistics may be written as

$$BIC = 2\ell_i(\hat{\boldsymbol{\theta}}_i) + \nu_i \ln(2RT), \tag{34}$$

where $\hat{\boldsymbol{\theta}}_i$ is the maximum likelihood estimator of the ν_i-dimensional parameter vector $\boldsymbol{\theta}_i$ of the i-th model, for $i = 1, \ldots, 27$, and RT is the number of complex observations. The criterion selects the model having the minimum BIC.

For the IPIX radar clutter data, the AR-GARCH-2D model with minimum BIC value is one of the models with better detection performance, i.e., $M = 3$, whose coefficient values are those of the process (32) used to generate synthetic data in the numerical analysis.

B. Performance Comparison

In this section, we consider three adaptive detectors and compare their performance with the selected AR-GARCH-2D detector. These are the generalized likelihood ratio test (GLRT) [2], the adaptive linear-quadratic (ALQ) detector [16] and the autoregressive generalized likelihood ratio (ARGLR) detector [4]. These detectors are obtained from the hypothesis test (14), with the same signal model $\mathbf{s}^r$ given in Section III, but different clutter models $\mathbf{v}^r$.

To estimate the clutter covariance matrix the GLRT and the ALQ detectors make use of K vectors $\{\mathbf{y}_n^r\}_{n=1}^K$ of secondary data from K range cells adjacent to the range cell under test. Secondary data are assumed to share the same statistics properties with the data $\mathbf{y}^r$ from the range cell under test. The GLRT can be written in the form [2]

$$\frac{|(\mathbf{p}^r)^H \hat{\mathbf{M}}_g^{-1} \mathbf{y}^r|^2}{\left[1 + \frac{1}{K}(\mathbf{y}^r)^H \hat{\mathbf{M}}_g^{-1} \mathbf{y}^r\right]\left[(\mathbf{p}^r)^H \hat{\mathbf{M}}_g^{-1} \mathbf{p}^r\right]} \underset{H_0}{\overset{H_1}{\gtrless}} \lambda, \tag{35}$$

where $\hat{\mathbf{M}}_g$ is the sample estimate of the clutter covariance matrix

$$\hat{\mathbf{M}}_g = \frac{1}{K} \sum_{n=1}^{K} \mathbf{y}_n^r (\mathbf{y}_n^r)^H. \tag{36}$$

The ALQ detector is given by [16]

$$\frac{|(\mathbf{p}^r)^H \hat{\mathbf{M}}_a^{-1} \mathbf{y}^r|^2}{\left[(\mathbf{y}^r)^H \hat{\mathbf{M}}_a^{-1} \mathbf{y}^r\right]\left[(\mathbf{p}^r)^H \hat{\mathbf{M}}_a^{-1} \mathbf{p}^r\right]} \underset{H_0}{\overset{H_1}{\gtrless}} 1 - e^{\lambda/N}, \tag{37}$$

where $\hat{\mathbf{M}}_a$ is the normalized sample covariance matrix estimate (NSCME) [15]

$$\hat{\mathbf{M}}_a = \frac{N}{K} \sum_{n=1}^{K} \frac{\mathbf{y}_n^r (\mathbf{y}_n^r)^H}{(\mathbf{y}_n^r)^H \mathbf{y}_n^r}. \tag{38}$$

The ARGLR is a detector that results from modeling the clutter as an AR process. This detector adjust itself to the environment using only the primary data and is given by [4]

$$\frac{(\mathbf{u} - \mathbf{Y}\hat{\mathbf{a}}_0)^H (\mathbf{u} - \mathbf{Y}\hat{\mathbf{a}}_0)}{(\mathbf{u} - \mathbf{Y}\hat{\mathbf{a}}_1)^H \mathbf{H}^H \mathbf{H} (\mathbf{u} - \mathbf{Y}\hat{\mathbf{a}}_1)} \underset{H_0}{\overset{H_1}{\gtrless}} e^{\lambda/N}, \tag{39}$$

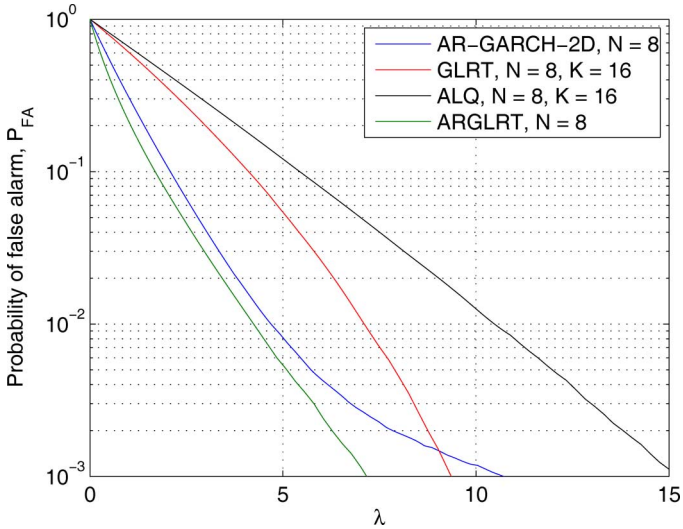

Fig. 8. Probability of false alarm versus threshold using IPIX radar clutter data.

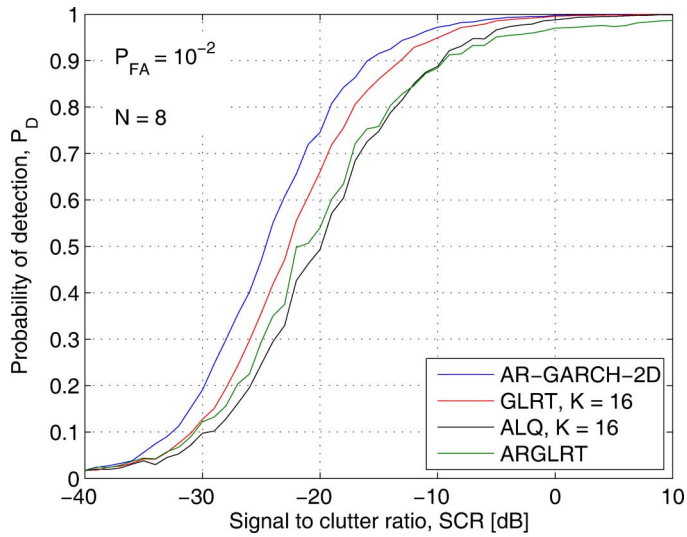

Fig. 9. Probability of detection versus signal to clutter ratio using IPIX radar clutter data and a synthetic target.

where the vectors $\hat{\mathbf{a}}_0$ and $\hat{\mathbf{a}}_1$ are $(\mathbf{Y}^H\mathbf{Y})^{-1}(\mathbf{Y}^H\mathbf{u})$ and $(\mathbf{Y}^H\mathbf{H}^H\mathbf{H}\mathbf{Y})^{-1}(\mathbf{Y}^H\mathbf{H}^H\mathbf{H}\mathbf{u})$ respectively, with

$$\mathbf{Y} = \begin{bmatrix} y_{rm} & \cdots & y_{r1} \\ \vdots & \ddots & \vdots \\ y_{r,N-1} & \cdots & y_{r,N-m} \end{bmatrix}, \tag{40}$$

$\mathbf{u} = [y_{r,m+1} \ \cdots \ y_{rN}]^T$, $\mathbf{H}$ the projection matrix of the null space of $\Upsilon = [1 \ e^{j\Omega} \ \cdots \ e^{j(N-m-1)\Omega}]^T$, and m the order of the AR process that models the clutter.

Fig. 8 shows the curves of the empirical probability of false alarm, P_{FA}, as a function of λ for the four detectors with $N = 8$ pulses. The curves were obtained using the *stare7* and *stare8* datasets of the IPIX radar. From these results we set λ for $P_{FA} = 10^{-2}$ for each detector and obtain the curves of P_D as a function of the SCR, with the signal model described in Section V-A. We also computed the empirical ROC for a $SCR = -15$ dB. Figs. 9 and 10 show the P_D vs. SCR curves and the ROC curves respectively. For the GLRT and the ALQ detectors we used $K = 16$ vectors of secondary data and for the ARGLR detector we considered a first order AR clutter model, i.e., $m = 1$, because its performance degrades when the order increases, since the coefficients are estimated poorly given the small number of primary data samples. The performance of our detector, based on the AR-GARCH-2D clutter model, is the best among all the tested alternatives, suggesting that the AR-GARCH-2D model matches better the sea clutter data than the other tested models. Note that the ARGLR and the ALQ detectors have almost the same performance and, the GLRT outperforms ALQ detector, as has been shown in [26].

VI. Discussion

We proposed the use of an autoregressive GARCH-2D process for better characterization of the sea clutter data. This model preserves the heavy tailed pdf of the GARCH processes and allows considering pulsewise correlation.

Based on the estimation method commonly used for GARCH processes we derived an estimation algorithm for the coefficients of the AR-GARCH-2D processes and we verified the estimator asymptotic properties by means of numerical simulations.

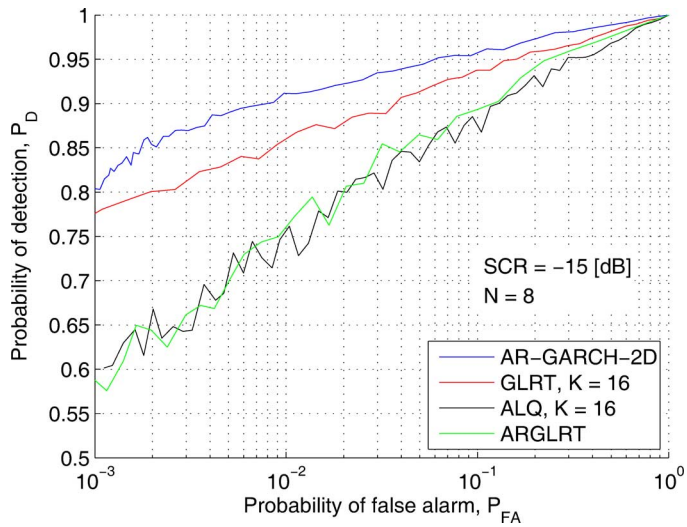

Fig. 10. Empirical ROC curves using IPIX radar clutter data and a synthetic target.

We also presented an adaptive detection algorithm based on this clutter model. One of the advantages of the AR-GARCH-2D detector is that it is a fast adaptive algorithm since the detection depends not only of the slow time neighborhood of the range cell under test, but also on the range or fast time neighborhood. Thus, it is able to pick the fast and heterogeneous behavior of the clutter.

We derived an expression of the false alarm probability for the AR-GARCH-2D detector. Given its mathematical complexity, we evaluated the detection probability by means of numerical simulations. We also analyzed how estimation errors in the coefficients affect the false alarm and detection probabilities. We observe that it is very robust in practical situations.

We evaluated the detection and false alarm probabilities by means of Monte Carlo simulations using real sea data and injecting a synthetic target, for the AR-GARCH-2D detector for different process orders. We showed that the detectors for which

the autoregressive order, M, is 2 or 3 present a better performance than the detectors for which M is 0 or 1, i.e., a higher detection probability with a lower false alarm rate. Then, we used a model selection criteria to choose one with an optimum compromise between complexity and fit.

We also compared the performance of the AR-GARCH-2D detector with the GLRT, the ALQ and the ARGLR detectors using actual clutter data. We showed that the proposed detector outperforms the other three detectors. The same behavior is observed for other datasets and for different number N of pulses involved in a decision. The GLRT is the second best detector, outperforming the ALQ detector designed assuming clutter is a compound-Gaussian process. In the case of the ARGLR detector, its performance degrades drastically when the number of integrated pulses decreases or the order of the AR model increases, since this detector adjusts itself to the environment using only primary data.

While we proposed and tested the AR-GARCH-2D clutter model for sea radar data, it should perform best in cases where the probability density function of the clutter has heavy tails, i.e., the clutter is impulsive. When the clutter is not impulsive, the α and β coefficients of the GARCH part of the model will not be statistically significant, and the detector will perform similarly to a detector for an AR Gaussian clutter model with secondary data. On the other hand, if the environment is such that there is no correlation between consecutive pulses, the AR part of the model will be negligible and the detector will work as a GARCH-2D detector. For non-impulsive uncorrelated clutter the detector further reduces to a detector for white-Gaussian clutter, albeit one with an unnecessarily large set of secondary data to estimate the clutter variance.

For a real time application, our detection algorithm has a practical amount of computational load. Two different computations must be performed: the estimation of the process coefficients, and the computation of the detection statistic. The latter does not involve a higher computational load, and unlike the other detectors it does not require solving any linear systems. Some terms in (30) involving the waveform p_{rt} can be precomputed, and it can be shown that for a model with $M = 3$, (30) and (31) can be solved with just $22N + 10$ real multiply-and-accumulate operations and a comparison. The estimation of the coefficients involves a much larger computational load, but it can be done as a batch process and the values do not need to be updated often. In fact, in the shown results, the estimation and detection was done with different datasets with 2 and 5 minutes delay. Similar coefficient values are obtained if the estimation is carried out with the *stare7* or *stare8* datasets, suggesting that only an important change in sea conditions would require an update of the coefficients.

A possible next step is to extend these ideas to use polarimetric information. This may be accomplished for example using a multivariate GARCH model [27].

Appendix A

In this appendix we present the expression for the constant ϕ_M appearing in the condition (10) for the unconditional variance of the AR-GARCH-2D process. The value of ϕ_M depends on the order M, thus we provide only the expressions for the values of M used in this work.

For $M = 0, 1, 2, 3$ the expressions of ϕ_M are respectively

$$\phi_0 = 0, \tag{41}$$

$$\phi_1 = |a_{01}|^2, \tag{42}$$

$$\phi_2 = \sum_{j=1}^{2} |a_{0j}|^2 + 2\mathrm{Re}\left\{ \frac{a_{01}a_{02}^*(a_{01} + a_{01}^* a_{02})}{1 - |a_{02}|^2} \right\}, \tag{43}$$

$$\begin{aligned}\phi_3 = \sum_{j=1}^{3} |a_{0j}|^2 + 2\mathrm{Re}\Bigg\{ & a_{01}a_{02}a_{03}^* + [a_{01}(a_{02}^* + a_{01}a_{03}^*) \\ & + a_{03}^*(a_{02} + a_{01}^* a_{03})] \\ & \cdot \frac{a_{01} + a_{02}^* a_{03} + \frac{(a_{01}^* + a_{02}a_{03}^*)(a_{02} + a_{01}^* a_{03})}{1 - |a_{03}|^2}}{1 - |a_{03}|^2 - \frac{|a_{02} + a_{01}^* a_{03}|^2}{1 - |a_{03}|^2}} \Bigg\},\end{aligned} \tag{44}$$

where * denotes complex conjugate and $\mathrm{Re}\{\cdot\}$ the real part of a complex number.

Appendix B

In this appendix we derive the value of γ that maximizes $f_1(\mathbf{y}^r/\psi_{r-1,N}; \{y_{r,t-M}\}_{t=1}^M)$ based on the first order necessary condition that it should satisfy to be a local maximizer [23]. The function $f_1(\mathbf{y}^r/\psi_{r-1,N}; \{y_{r,t-M}\}_{t=1}^M)$ is a real-valued function of a complex parameter γ. Since $f_1(\mathbf{y}^r/\psi_{r-1,N}; \{y_{r,t-M}\}_{t=1}^M)$ is analytic with respect to γ and γ^* a necessary and sufficient condition for $f_1(\mathbf{y}^r/\psi_{r-1,N}; \{y_{r,t-M}\}_{t=1}^M)$ to have a stationary point is

$$\frac{\partial f_1(\mathbf{y}^r/\psi_{r-1,N}; \{y_{r,t-M}\}_{t=1}^M)}{\partial \gamma} = 0, \tag{45}$$

where γ^* is treated as a constant in the partial derivative [28].

Equivalently we can find the stationary points of $\ln(f_1(\mathbf{y}^r/\psi_{r-1,N}; \{y_{r,t-M}\}_{t=1}^M))$, because the $\ln\{\cdot\}$ is a monotonically increasing function. Once we obtain $f_1(\mathbf{y}^r/\psi_{r-1,N}; \{y_{r,t-M}\}_{t=1}^M)$ replacing (19) in (15), we take $\ln\{\cdot\}$. Then, from (19) the derivative of $\ln(f_1(\mathbf{y}^r/\psi_{r-1,N}; \{y_{r,t-M}\}_{t=1}^M))$, with respect to γ is given by

$$\frac{\partial \ln(f_1)}{\partial \gamma} = \sum_{t=1}^{N} \frac{1}{\sigma_{rt}^2} \Delta p_{rt} \left(\Delta y_{rt} - \gamma \Delta p_{rt}\right)^*, \tag{46}$$

where we denote $\Delta p_{rt} = p_{rt} - \sum_{j=1}^M a_{0j} p_{r,t-j}$ and $\Delta y_{rt} = y_{rt} - \sum_{j=1}^M a_{0j} y_{r,t-j}$. Thus, (46) is zero when $\gamma = \hat{\gamma}$ resulting in

$$\sum_{t=1}^{N} \frac{1}{\sigma_{rt}^2} \Delta p_{rt} \left(\Delta y_{rt}\right)^* = \hat{\gamma}^* \sum_{t=1}^{N} \frac{1}{\sigma_{rt}^2} |\Delta p_{rt}|^2. \tag{47}$$

From (47) we obtain the expression of $\hat{\gamma}$ given in (20).

References

[1] I. Reed, J. Mallett, and L. Brennan, "Rapid convergence rate in adaptive arrays," *IEEE Trans. Aerosp. Electron. Syst.*, vol. AES-10, no. 6, pp. 853–863, Nov. 1974.

[2] E. J. Kelly, "An adaptive detection algorithm," *IEEE Trans. Aerosp. Electron. Syst.*, vol. AES-22, no. 1, pp. 115–127, Mar. 1986.

[3] S. Bose and A. Steinhardt, "A maximal invariant framework for adaptive detection with structured and unstructured covariance matrices," *IEEE Trans. Signal Process.*, vol. 43, no. 9, pp. 2164–2175, Sep. 1995.

[4] A. Sheikhi, M. Nayebi, and M. Aref, "Adaptive detection algorithm for radar signals in autoregressive interference," *Proc. Inst. Electr. Eng. —Radar, Sonar, Navig.*, vol. 145, no. 5, pp. 309–314, Oct. 1998.
[5] S. Kraut and L. Scharf, "The CFAR adaptive subspace detector is a scale-invariant GLRT," *IEEE Trans. Signal Process.*, vol. 47, no. 9, pp. 2538–2541, Sep. 1999.
[6] S. Haykin, C. Krasnor, T. J. Nohara, B. W. Currie, and D. Hamburger, "A coherent dual-polarized radar for studying the ocean environment," *IEEE Trans. Geosci. Remote Sens.*, vol. 29, no. 1, pp. 189–191, Jan. 1991.
[7] A. Farina, F. Gini, M. Greco, and L. Verrazzani, "High resolution sea clutter data: Statistical analysis of recorded live data," *Proc. Inst. Electr. Eng.—Radar, Sonar, Navig.*, vol. 144, no. 3, pp. 121–130, Jun. 1997.
[8] K. Sangston and K. Gerlach, "Coherent detection of radar targets in a non-Gaussian background," *IEEE Trans. Aerosp. Electron. Syst.*, vol. 30, no. 2, pp. 330–340, Apr. 1994.
[9] D. A. Shnidman, "Generalized radar clutter model," *IEEE Trans. Aerosp. Electron. Syst.*, vol. 35, no. 3, pp. 857–865, Jul. 1999.
[10] V. Anastassopoulos, G. A. Lampropoulos, A. Drosopoulos, and M. Rey, "High resolution radar clutter statistics," *IEEE Trans. Aerosp. Electron. Syst.*, vol. 35, no. 1, pp. 43–60, Jan. 1999.
[11] X. Shang and H. Song, "Radar detection based on compound-Gaussian model with inverse gamma texture," *IET Radar, Sonar, Navigat.*, vol. 5, no. 3, pp. 315–321, Mar. 2011.
[12] K. Sangston, F. Gini, and M. Greco, "Coherent radar target detection in heavy-tailed compound-Gaussian clutter," *IEEE Trans. Aerosp. Electron. Syst.*, vol. 48, no. 1, pp. 64–77, Jan. 2012.
[13] E. Conte and M. Longo, "Characterisation of radar clutter as a spherically invariant random process," *Proc. Inst. Electr. Eng.—Commun., Radar, Signal Process.*, vol. 134, no. 2, pp. 191–197, Apr. 1987.
[14] E. Conte, M. Lops, and G. Ricci, "Adaptive matched filter detection in spherically invariant noise," *IEEE Signal Process. Lett.*, vol. 3, no. 8, pp. 248–250, Aug. 1996.
[15] F. Gini, M. Greco, and L. Verrazzani, "Detection problem in mixed clutter environment as a Gaussian problem by adaptive preprocessing," *Electron. Lett.*, vol. 31, no. 14, pp. 1189–1190, Jul. 1995.
[16] F. Gini and M. V. Greco, "Suboptimum approach to adaptive coherent radar detection in compound-Gaussian clutter," *IEEE Trans. Aerosp. Electron. Syst.*, vol. 35, no. 3, pp. 1095–1104, Jul. 1999.
[17] J. P. Pascual, N. von Ellenrieder, M. Hurtado, and C. H. Muravchik, "Radar detection algorithm for GARCH clutter model," *Digit. Signal Process.*, vol. 23, no. 4, pp. 1255–1264, Jul. 2013.
[18] T. Bollerslev, "Generalized autoregressive conditional heteroscedasticity," *J. Econometr.*, vol. 31, no. 3, pp. 307–327, Feb. 1986.
[19] M. Amirmazlaghani, H. Amindavar, and A. Moghaddamjoo, "Speckle suppression in SAR images using the 2-D GARCH model," *IEEE Trans. Image Process.*, vol. 18, no. 2, pp. 250–259, Feb. 2009.
[20] A. Noiboar and I. Cohen, "Anomaly detection based on wavelet domain GARCH random field modeling," *IEEE Trans. Geosci. Remote Sens.*, vol. 45, no. 5, pp. 1361–1373, May 2007.
[21] M. Greco, F. Bordoni, and F. Gini, "X-band sea-clutter nonstationarity: Influence of long waves," *IEEE J. Ocean. Eng.*, vol. 29, no. 2, pp. 269–283, Apr. 2004.
[22] S. M. Kay, *Fundamentals of Statistical Signal Processing, Detection Theory*. Upper Saddle River, NJ, USA: Prentice-Hall, 1998.
[23] R. Fletcher, *Practical Methods of Optimization*. New York, NY, USA: Wiley, 1987.
[24] M. A. Richards, *Fundamentals of Radar Signal Processing*. New York, NY, USA: McGraw-Hill, 2005.
[25] S. Konishi and G. Kitagawa, *Information Criteria and Statistical Modeling*. New York, NY, USA: Springer, 2008.
[26] F. Gini, M. Greco, M. Diani, and L. Verrazzani, "Performance analysis of two adaptive radar detectors against non-Gaussian real sea clutter data," *IEEE Trans. Aerosp. Electron. Syst.*, vol. 36, no. 4, pp. 1429–1439, Aug. 2000.
[27] L. Bauwens, S. Laurent, and J. Rombouts, "Multivariate GARCH models: A survey," *J. Appl. Econometr.*, vol. 21, no. 1, pp. 79–109, Feb. 2006.
[28] D. H. Brandwood, "A complex gradient operator and its application in adaptive array theory," *Proc. Inst. Electr.—F, Commun., Radar, Signal Process.*, vol. 130, no. 1, pp. 11–16, Feb. 1983.

Juan P. Pascual received his Eng. degree in Electronics Engineering from the Universidad Nacional de La Plata (UNLP), Buenos Aires, Argentina, in 2006. He is currently a Ph.D. candidate in the UNLP. His research interests focus on statistical and array signal processing with radar and communication applications.

Nicolás von Ellenrieder (S'96–M'06) is a Professor at the Universidad Nacional de La Plata, were he received his Eng. (1998) and Ph.D. (2005) degrees. His postdoctoral experience includes research visits to the Washington University in St. Louis (2006), the Cuban Neuroscience Center (2006), and the Montreal Neurological Institute of McGill University (2010, 2013). His research interests include statistical and digital signal processing with applications in the fields of biomedicine and radar.

Martín Hurtado (M'11) received the B.Eng. and M.Sc. degrees in electrical engineering from the National University of La Plata, Argentina, in 1996 and 2001, respectively. He received his Ph.D. degree in electrical engineering from Washington University in St. Louis in 2007. Currently, he is a research associate of the National Council of Scientific and Technical Research of Argentina and an adjunct professor in the Department of Electrical Engineering at National University of La Plata. His research interests are in the area of statistical signal processing, detection and estimation theory, and their applications in sensor arrays, communications, and remote sensing systems.

Carlos H. Muravchik (S'81–M'83–SM'99) graduated in Electronics from the National University of La Plata, Argentina, in 1973. He received the M.Sc. in Statistics (1983) and the M.Sc. (1980) and Ph.D. (1983) degrees in Electrical Engineering, from Stanford University, Stanford, CA. He is a Professor at the Department of the Electrical Engineering of the National University of La Plata and a member of the Comisión de Investigaciones Cientificas de la Pcia. de Buenos Aires. He was a Visiting Professor to Yale University in 1983 and 1994, to the University of Illinois at Chicago in 1996, 1997, 1999, and 2003 and to Washington University in St. Louis in 2006 and 2010. Since 1999 he is a member of the Advisory Board of the journal *Latin American Applied Research* and was an Associate Editor of the IEEE TRANSACTIONS ON SIGNAL PROCESSING (2003–2006). His research interests are in the area of statistical and array signal processing with biomedical, communications and control applications, and in nonlinear control systems.